PREPARATION OF CITRONELLAL NANOCAPSULES AND STUDY OF ANTIBACTERIAL AND MOSQUITO REPELLENT PROPERTIES OF CITRONELLAL FUCTIONALIZED LYOCELL FIBER

FEIYAN ZHANG, XIAOLI ZHANG, LIRONG YAO and LUOLAN WANG

School of Textile and Clothing, Nantong University, Nantong, 226019, China
✉ *Corresponding author: X. Zhang, zhangxl@ntu.edu.cn*

Received October 14, 2023

The encapsulation of botanical compounds (such as citronellal) can be used to increase their efficiency and stability for functionalizing textile materials. In this study, the citronellal nanocapsules (CNC) with citronella oil as the core material and isophorone diisocyanate (IPDI) as the shell material were prepared and characterized. Factors, including core-to-shell ratio, single-phase ratios, emulsification time, as well as polymerization time and temperature, were investigated to determine the optimal process for the preparation of CNC. The average particle size of the prepared CNC was about several hundred nanometers, with uniform particle size distribution. Further, composite Lyocell fibers were prepared by the wet spinning process of co-blending CNC with Lyocell spinning stock. Evaluations were made of the biological activity of CNC towards mosquitoes, as well as *E. coli* and *S. aureus*, showing excellent mosquito repelling rate, of more than 90%, and an inhibition rate of 97.72% towards *S. aureus*.

Keywords: citronellal nanocapsules, interfacial polymerization method, functional Lyocell fiber, antibacterial and mosquito repellent effect

INTRODUCTION

Global health threats, primarily due to mosquito-borne diseases, can have major social and economic impacts on communities.[1] A mosquito-borne disease remains a challenge since there is no vaccine to prevent it, while further drug resistance is another growing health threat. Under these circumstances, process control plays a vital role and often remains the only way to prevent disease outbreaks. The control and elimination of mosquitoes rely upon indoor mosquito spray or bed nets. However, mosquito sprays can be toxic to humans, especially infants,[2] and are also very inconvenient to be used outdoors. With increasing awareness of ecological and health safety, bio-pesticides have become a major focus as an efficient tool against mosquitoes. Plant essential oils have unique chemicals, with anti-mosquito vector activity, which kill or repel mosquito, but are safe to other species, and are widely used as an alternative to commercial synthetic insecticides.[3]

Although the use of plant-derived botanical mosquito repellents (essential oils and crude plant extracts) has occupied a key place in mosquito management, the application of botanicals is still limited because of poor water solubility, and further feasibility of plant-based products is not ensured because of volatility, degradation, and stability issues. In addition, most essential oils cannot come into direct contact with the skin, causing skin irritation, or because of the possibility of skin penetration.[4,5] Microcapsules act as a storage container, in which the repellent can be stored and slowly released when in the environment, increasing the duration of its action, while reducing its exposure to direct contact with the skin, thus reducing skin penetration.[3,6,7] Microencapsulation by the interfacial polymerization method is simple and low-cost, and the product can be controlled by changing the reaction parameters.[8]

Lyocell, a cellulose fiber, has been widely utilized in textiles due to its soft, smooth, environmentally friendly, and breathable properties.[9] Such fibers can also be adapted to develop specific functional textiles. Cell Solution® fibers are natural cellulosic man-made fibers produced by an environmentally friendly and safe new solvent process, endowed with a specific functionality. Cell Solution® fibers offer insecticidal protection due to the synthetic chemical permethrin embedded into the fibers. Other attempts to develop anti-mosquito fibers have also been reported, relying on adding synthetic anti-mosquito finishing agents to the fiber by the spinning technology.[10]

In this work, we present the preparation and characterization of citronellal nanocapsules (CNC) and further formation of Lyocell fiber with the inclusion of such CNC by the wet spinning process. The average particle size of the fabricated citronellal nanocapsules was 220.5 nm, with uniform particle size distribution. The functional fibers were tested in terms of their repellent and antibacterial properties. The results showed a mosquito repellent rate of 93%, and an inhibition rate to *Staphylococcus aureus* of 97.72%. Therefore, after the addition of citronellal nanocapsules, the Lyocell fiber was provided with an excellent multifunctional profile, exhibiting both mosquito-repellent function and antibacterial activity.

EXPERIMENTAL

Materials

The citronella essential oil (CO) was for the present study was industrial grade, received from Green Source Natural Flavor Oil Refinery, Qingyuan District, Ji'an City. The following chemicals were used: glyceryl octanoate (GTCC, 99%, Shandong Yusuo Chemical Technology Co., Ltd.), isophorone diisocyanate (IPDI, industrial grade, Shanghai Runjie Chemical Reagent Co., Ltd.), sodium dodecyl sulfate (SDS, 10%, Shanghai Runjie Chemical Reagent Co., Ltd.), tetramethylethylenediamine (TEMED, analytically pure, Shanghai Runjie Chemical Reagent Co., Ltd.), ethylene glycol (EG, analytically pure, Shanghai Runjie Chemical Reagent Co. Ltd.), polyethylene glycol octyl phenyl ether (OP emulsifier, chemically pure, Jiangsu Qingsheng Functional Chemical Co., Ltd.). Lyocell fiber was obtained from Lenzing Group, Austria.

For the antibacterial tests, nutritional broth (bioreagent, Hangzhou Best Biotechnology Co.), nutrient agar (bioreagent, Hangzhou Best Biotechnology Co., Ltd.), phosphate buffer (bioreagent, Hangzhou Best Biotechnology Co., Ltd.), *Escherichia coli* (*E. coli*, ATCC25922, Shanghai LUMI Technology Co., Ltd.), *Staphylococcus aureus* (*S. aureus*, CMCC (B) 26003, Shanghai LUMI Technology Co., Ltd.), deionized water (DI, prepared in the laboratory), and anhydrous ethanol (analytical purity, Jiangsu Qingsheng Functional Chemical Co., Ltd.) were used.

Preparation of citronellal nanocapsules

Citronella aldehyde was encapsulated by interfacial polymerization and the flow chart of the preparation is shown in Figure 1. The total mass of the control system was 50 g. An appropriate amount of deionized water and a certain amount of porogenic agent EG were added to the 10% SDS solution (10 g), under stirring, resulting in the aqueous phase. The appropriate amount of monomer IPDI was added to 15 g of core material (CO/GTCC), under stirring, resulting in the oil phase. Then, the aqueous phase and oil phase were mixed and placed in an ice-water bath. The resulting mixture was emulsified under the action of an ultrasonic cleaner for 30 min to generate an O/W type nanoemulsion.

The nanoemulsions were placed in a constant temperature water bath with mechanical stirring and the appropriate amount of catalyst TEMED was added drop by drop to react at 60 °C for 4 h. The OP emulsifier was added after the reaction and stirred well. The effects of core-to-shell ratio, single-phase ratio, emulsification time, polymerization time and temperature on the preparation of CNC were investigated and the optimal process was determined.

Lyocell fiber with mosquito repellent finish

The CNC made by the optimum process were added to the spinning solution of Lyocell, and Lyocell fiber with mosquito repellent function was obtained by wet spinning (this process was performed at the Beijing Institute of Textile Science). The CO content used in the formulation was 5%, and the doping amount of the spinning silk stock solution was 22%.

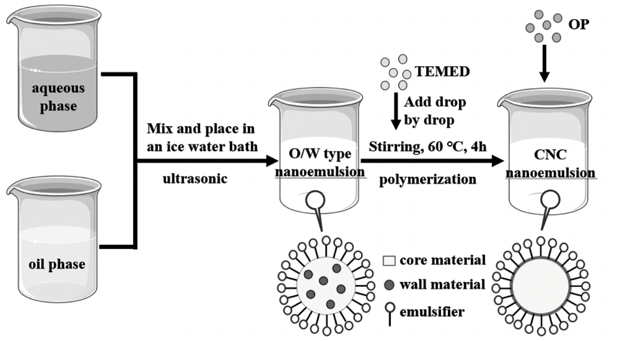

Figure 1: Flow chart of citronellal nanocapsule preparation

Characterization

Morphology and particle size of nanocapsules

The distribution and morphology of CNC emulsion particles at different magnifications were observed with a DN-10B biological microscope, and the size and distribution of the produced citronellal nanocapsules were measured with a 90 Plus Zeta Nanoparticle Size Analyzer.

Functional Lyocell fiber performance

The developed Lyocell fibers were characterized in terms of their tensile properties, morphology, chemical structures and thermal behavior.

The tensile properties of neat Lyocell fibers and functional Lyocell fibers, with incorporated CNC, were tested with an YG001D Single Fiber Strength Meter.

The morphology of both types of Lyocell fibers was observed using a Gemini SEM 300 Field Emission Scanning Electron Microscope (Carl Zeiss, Germany), at an accelerating voltage of 5 kV.

For the Fourier transform infrared spectroscopy (ATR-FTIR) study, a Nicolet IS50 Infrared Spectrometer (Thermo, USA) was used for spectral scanning of the Lyocell fibers in the range of 4000~500 cm^{-1} to characterize their chemical structures.

Also, synchronous thermal analysis (STA) was performed on the fibers to examine their thermal decomposition. For this purpose, an STA 449 F5 Simultaneous Thermal Analyzer (Netzsch, Germany) was used, at a heating rate of 10 °C/min and a heating range of 30 °C~800 °C, under airflow of high purity nitrogen.

Mosquito repelling performance test

The mosquito-repelling performance of fibers was measured at the Institute of Parasitic Disease Prevention and Control, of the Chinese Center for Disease Control and Prevention. The samples were tested according to GB/T 28408-2012 “Protective clothing, insect-proof protective clothing” and GB/T 30126-2013 “Testing and evaluation of the mosquito-proof performance of textiles”.

Aedes albopictus female adults (about 60) were introduced into a mosquito cage (33 cm × 33 cm × 33 cm). The specimen was attached to the human body or a blood donor. The number of mosquitoes stopping within the specified time on the test sample and the control sample surface was counted.

The tests were replicated and average data were used to calculate the repellent rate according to the following formula:

$$P = (N - K)/N \times 100\% \quad (1)$$

where P – repellent rate, %; K – total number of mosquitoes stopping on the anti-mosquito treated fabric; N – total number of mosquitoes stopping on the control fabric. P > 70% is rated as grade A (very strong repellent effect), 50% < P < 70% is rated as grade B (good repellent effect), 30% < P < 50% is rated as grade C (moderate repellent effect).

Antibacterial performance test

The antibacterial performance test was carried out according to the improved GB/T20944.3-2008 “Evaluation of Antibacterial Performance of Textiles Part 3: Oscillation Method” to test the antibacterial performance of CNC. Gram-negative *E. coli* and gram-positive *S. aureus* were selected as the test strains. The inhibition rate was calculated as follows:

$$X = (B - A)/B \times 100\% \quad (2)$$

where X – rate of bacterial inhibition, %; A – number of colonies in the Petri dish of the test sample; B – number of colonies in the control Petri dishes.

RESULTS AND DISCUSSION

Optimization of the preparation process of citronellal nano/microcapsules and characterization

Core-to-shell ratio

According to the above-mentioned preparation method, the effect of core-to-shell ratio on CNC preparation was explored. For this, 15 g of core material was weighed, and the ratio of the core material to the shell material was varied (1:2, 1:1, 2:1, 3:1, 4:1, 5:1, 6:1, 7:1), while the other conditions were kept constant, to synthesize CNC.

Microscopy images of nanocapsules prepared with different core-to-shell ratios are shown in Figure 2. It may be noticed that, when the core-shell ratios were 1:2 and 1:1, there were very few nanocapsule emulsion particles in the solution, with large particle sizes and uneven particle size distribution. It is because when the core shell ratio is small, the excess IPDI is encapsulated in the nanocapsules and cannot continue to react. So, fewer nanocapsules are formed. When the core-shell ratios were 2:1, 3:1, 4:1, and 5:1, there were obvious uncoated oil droplets in the solution. As the core-to-shell ratio increases, IPDI decreases, resulting in a large number of emulsion particles in the solution. Moreover, the distribution is more uniform, the particle size distribution being narrower, and the particle size decreases. However, when the core-to-shell ratio increases to 7:1, the excess core material leads to incomplete encapsulation, the difference in the size of emulsion particles increases, there is an obvious agglomeration phenomenon, and insufficient IPDI will affect the mechanical properties of the capsule shell layer. Therefore, the optimal core-to-shell ratio was determined as 6:1.

Core material ratio

The effect of core ratios (CO to GTCC mass ratio) was investigated. As shown in Figure 3, when the mass ratio of CO to GTCC is 1:3, the particle size of the emulsion in the solution varies widely and the agglomeration phenomenon is obvious. As the mass ratio of CO to GTCC increases, the agglomeration phenomenon and average particle size decrease, while the distribution of emulsion particles in the solution is more uniform and dense. The system tends to be stable, which can be explained by the fact that excessive GTCC tends to make the emulsification system less stable. When the mass ratio of CO to GTCC reaches 3:1, the morphology and particle size of nanocapsules almost reach the optimum. Therefore, the mass ratio of CO to GTCC was selected as 3:1.

Ethylene glycol dosage

The core material is released from the capsules by reacting EG with polyurethane as a porogenic agent to create voids on the surface of the polyurethane film. Therefore, the amount of EG is a key factor for the release rate of nanocapsules. Here, the effect of EG amount on CNC preparation was explored by varying the mass of IPDI to EG as 2:1, 3:1, 4:1, 5:1, and 6:1.

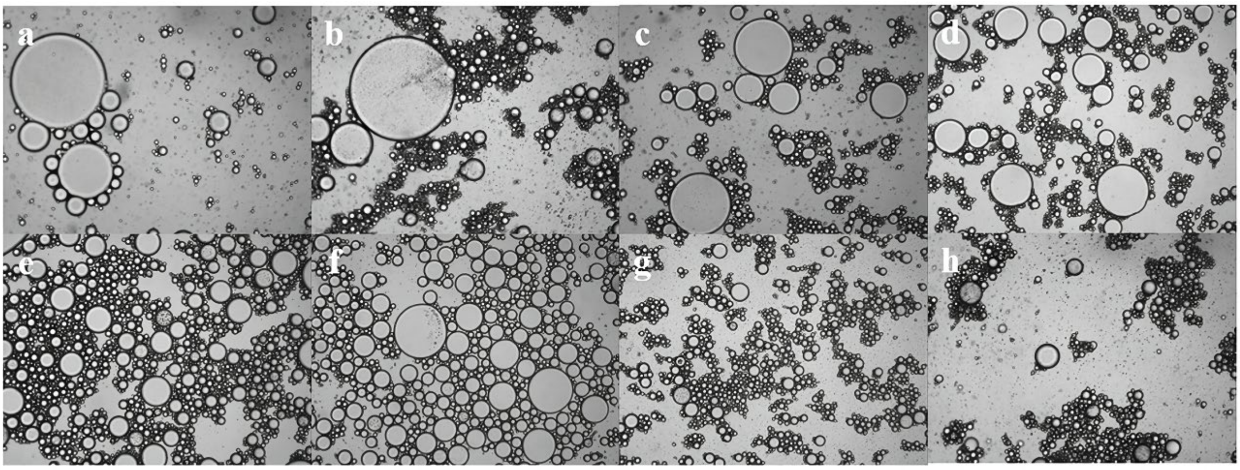

Figure 2: Microscopy images of nanocapsules prepared with different core-to- shell ratios (a-1:2; b-1:1; c-2:1; d-3:1; e-4:1; f-5:1; g-6:1; h-7:1)

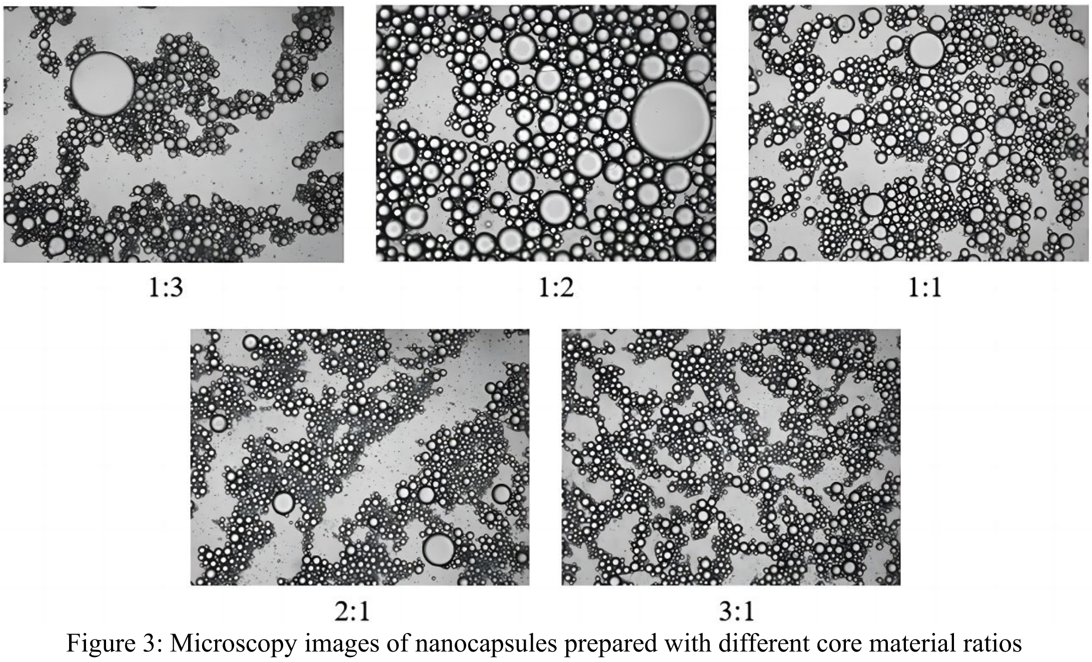

Figure 3: Microscopy images of nanocapsules prepared with different core material ratios

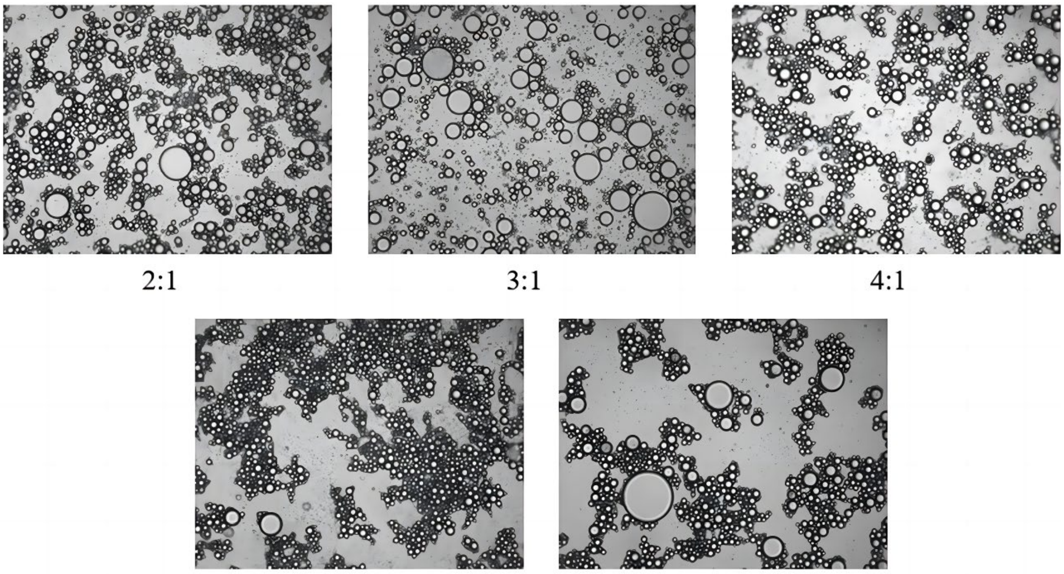

Figure 4: Microscopy images of nanocapsules prepared with different EG dosages

As shown in Figure 4, when the mass ratio of IPDI to EG is 2:1, the particle size distribution of the emulsion particles in the solution is uneven. It is because EG has a good dispersion effect on the shell material, owing to the hydrophilic group, but an overdose can cause the stability of nanocapsules to decrease, leading to the agglomeration phenomenon. As the mass ratio of IPDI to EG increases, when the mass ratio of IPDI to EG is 4:1, the particle size of emulsion particles is small and the distribution is more uniform. As the mass ratio of IPDI to EG continues to increase, the particle size of the emulsion and the difference of particle size also increase. The dispersion is weak because of the lower amount of EG, resulting in the small uniformity of distribution and the agglomeration phenomenon. Therefore, the mass ratio of IPDI to EG was selected as 4:1.

Amount of tetramethylethylenediamine

With TEMED as the catalyst, -NCO and H_2O in IPDI react at the water/oil two-phase interface to form a network-like polymer. As the reaction continues, the two-phase monomers at the interface decrease, and the unreacted monomers continuously diffuse to the interface to participate in polymerization, forming a polymer film layer to encapsulate the oil-phase core material. The mass fraction of TEMED was varied as follows: 5%, 7.5%, 10%, 12.5%, and 15% of the shell material. As shown in Figure 5, when the mass fraction of TEMED to IPDI is 5% and 7.5%, the amount of TEMED is too small, resulting in the thermal movement collision and merging of the emulsion particles, and therefore, the particle size distribution is not uniform. When the mass fraction increases to 10%, the emulsion particle size decreases and the particle size distribution is more uniform. With the increase of TEMED dosage, the excess TEMED constantly reacts with IPDI, the stability of the capsule shell of nanocapsules increases and agglomeration occurs, while the particle size of nanocapsules and the difference of particle size also increase. Therefore, the mass fraction of TEMED to the shell material was selected as 10%.

Emulsification time

The emulsification time was varied as: 10 min, 20 min, 30 min, 40 min and 50 min. The analysis in Figure 6 shows that, when the emulsification time is 10 min and 20 min, the particle size distribution of the nanocapsule emulsion particles in the solution is uneven, and there is an agglomeration phenomenon, probably because the emulsification time is short, and the stability of the system is low, resulting in uneven particle size distribution of emulsion particles. When the emulsification time reaches 30 min, the emulsification system is relatively stable, the particle size of emulsion particles decreases, and the particle size distribution is uniform. When the emulsification time continues to increase, the particle size of emulsion particles increases, the difference in particle size increases, and the number of emulsion particles decreases, probably because the emulsification time is too long and the emulsion breaking phenomenon occurs, which leads to the re-gathering of already dispersed droplets, the capsule particle size increases, and the agglomeration phenomenon occurs. Therefore, the emulsification time was selected as 30 min.

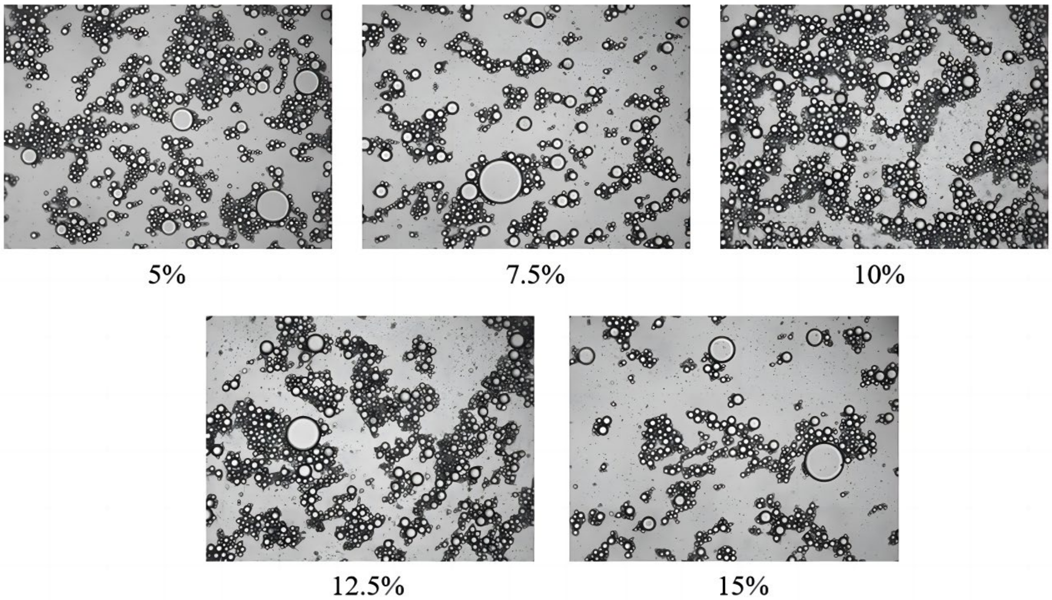

Figure 5: Microscopy images of nanocapsules prepared with different TEMED dosages

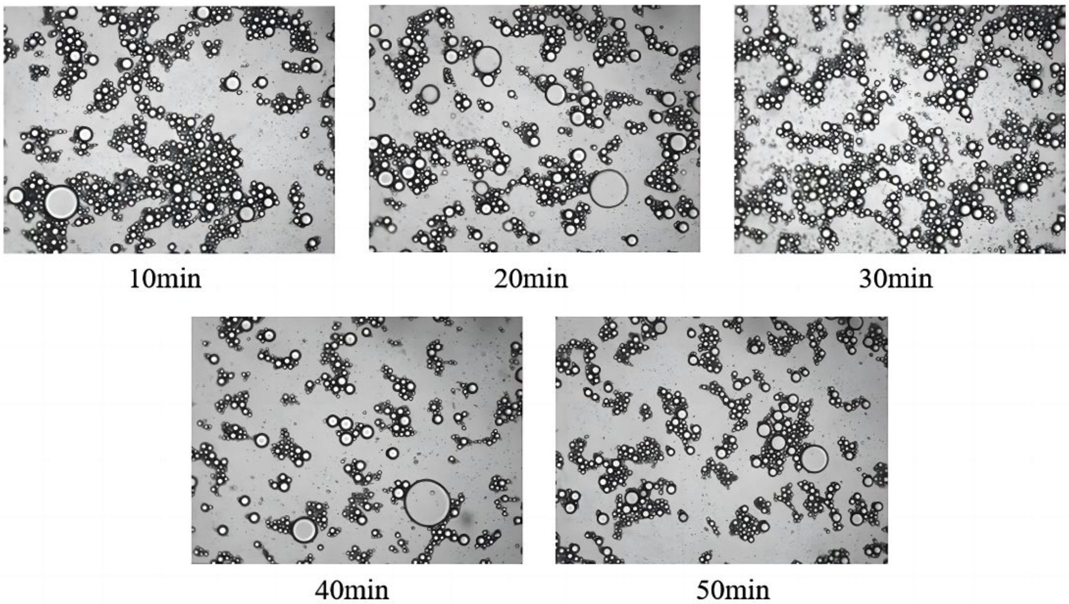

Figure 6: Microscopy images of nanocapsules prepared at different emulsification times

Polymerization temperature

The polymerization temperature was varied as 40, 50, 60, 70 and 80 °C. The analysis of Figure 7 reveals that the particle size of CNC first decreases and then increases with the increase of polymerization temperature. When the polymerization temperature is less than 60 °C, the reaction rate is slow because the reaction temperature is too low, IPDI has not yet wrapped the core material in time, and at the same time, the irregular movement of emulsion particles is slow, and they attract each other and gather into large particles, so the particle size of emulsion particles is large and the particle size distribution is not uniform. When the polymerization temperature reaches 60 °C, the reaction rate is accelerated, the average particle size of capsules is small and the particle size distribution is uniform. As the polymerization temperature continues to rise, the irregular motion of nanocapsule emulsion particles is intense and particles collide with each other, which leads to the agglomeration of nanocapsule particles, and thus, the difference of particle size increases. When the temperature reaches 80 °C, the agglomeration phenomenon is obvious. Therefore, the polymerization temperature was selected as 60 °C.

Polymerization time

The polymerization time was varied as follows: 1 h, 2 h, 3 h, 4 h, and 5 h, to explore the effect of polymerization time on microcapsules. From the analysis of Figure 8, it can be seen that when the polymerization time is less than 4 h, there is no obvious change in the particle size of emulsion particles in the solution, and the particle size distribution is uneven, probably because the polymerization time is too short, the polymerization reaction occurs incompletely, the encapsulation rate is not high, the capsule shell of nanocapsules is fragile, and the core material easily leaks out. When the polymerization time reaches 4 h, the average particle size of the emulsion particles decreases and the particle size distribution is uniform. However, when the polymerization time is greater than 4 h, due to the long reaction time, the phenomenon of emulsion breaking and agglomeration occurs under the action of high-speed stirring, the average particle size of emulsion particles increases and the difference of particle size becomes larger. Therefore, the polymerization time of 4 h was selected.

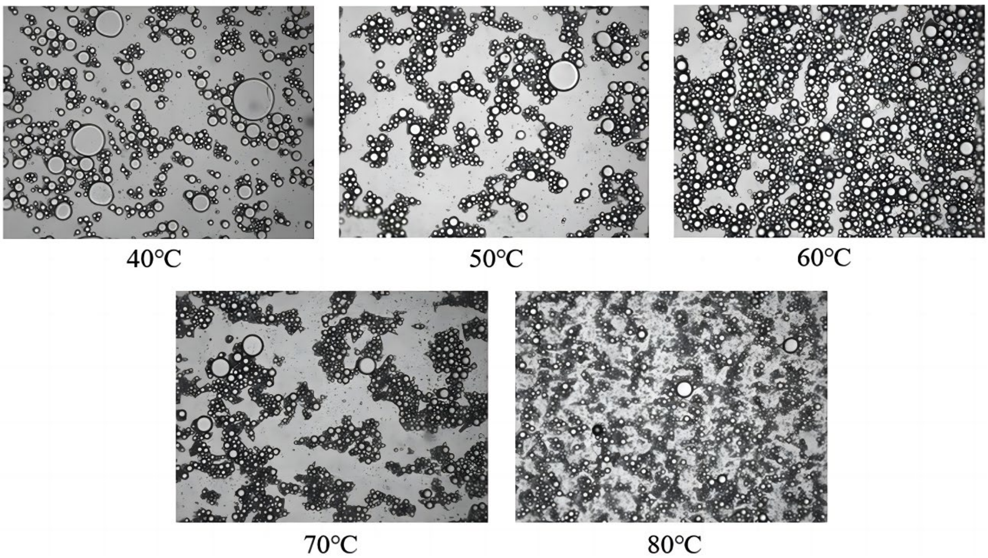

Figure 7: Microscopy images of nanocapsules prepared at different polymerization temperatures

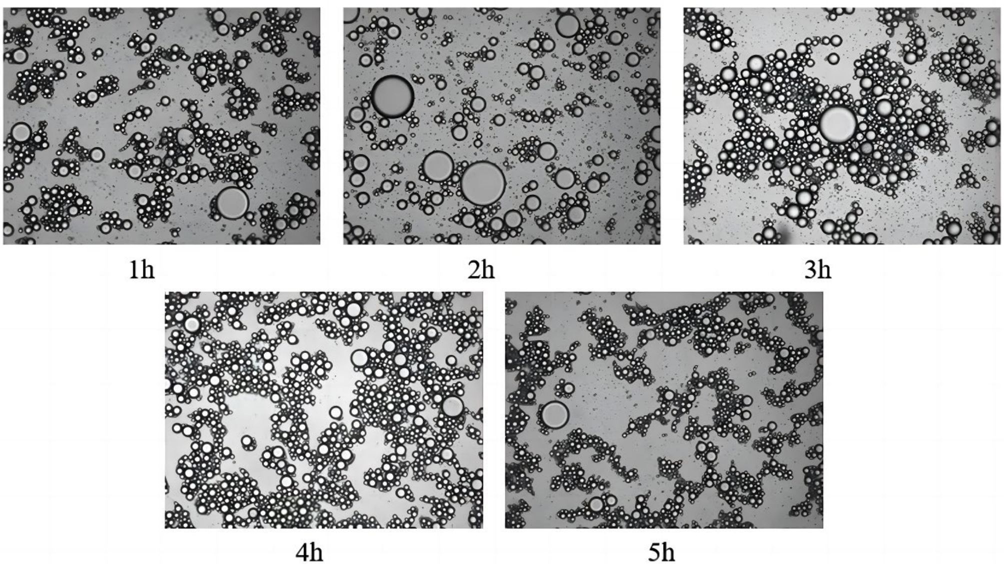

Figure 8: Microscopy images of nanocapsules prepared at different polymerization times

Particle size and distribution of citronellal nanocapsules

The particle size distribution of CNC prepared under the optimal process conditions is shown in Figure 9. From the analysis of Figure 9, it can be seen that the CNC particle size is in the nanometer range and is normally distributed, mainly between 100 and 500 nm, with an average particle size of 220.5 nm.

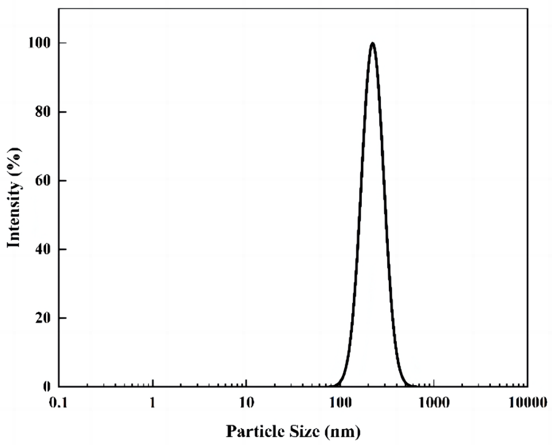

Figure 9: Particle size distribution of citronellal nanocapsules

Table 1
Tensile testing of neat and functional Lyocell fibers

Property	Neat Lyocell fiber	Functional Lyocell fiber
Breaking strength, cN	109.09	82.81
Elongation at break, %	2.43	1.54

Characterization of mosquito repellent Lyocell fiber performance

Tensile performance of fiber

The average breaking strength and elongation at break results of neat Lyocell fiber and mosquito-repellent Lyocell fiber with CNC are shown in Table 1.

From the data in Table 1, it can be seen that after the addition of CNC, the breaking strength of Lyocell fibers decreased by 24.09% and the elongation at break decreased by 36.63%. This is because the spinning stock contains 22% nanocapsules with high doping, which has a great impact on the mechanical properties of the fibers. The addition of CNC breaks the regular arrangement of Lyocell fiber macromolecules, which changes the aggregated state structure and decreases the crystallinity. In addition, CNC hinders the hydrogen bonding between cellulose molecules, which reduces the degree of cross-linking and decreases the fiber-breaking strength and elongation at break.

Microscopic morphology analysis of fiber

Transverse and longitudinal SEM images of neat Lyocell fibers and mosquito-repellent functional Lyocell fibers are shown for comparison in Figure 10. In the longitudinal direction, the surface of neat Lyocell fiber is smooth, while the surface of functional Lyocell fiber with CNC is slightly rough with fine particles, which may be due to the increase of tiny particles on the surface due to the co-blending of nanocapsules with the spinning stock. Transversely, the cross-section of neat Lyocell fibers was denser, while the functional Lyocell fibers had holes in the transverse cross-section, which might be due to the holes left by the rupture of the nanocapsules.

Fourier infrared spectroscopy analysis

From Figure 11, it can be observed that there is a significant broad absorption peak at 3357 cm^{-1} and a strong absorption peak at 1017 cm^{-1} corresponding to the stretching vibration of -OH and the stretching vibration of C-O, which is considered to indicate incomplete reaction of EG. The absorption peak at 1633 cm^{-1} is attributed to the stretching vibration absorption peak of carbonyl C=O, which is due to the reaction of IPDI with water and TEMED, forming an amide bond (-CO-NH-), but the stretching vibration of N-H is not obvious due to the low content of the shell material. In summary, the presence of CNC in functional Lyocell fibers was proved.

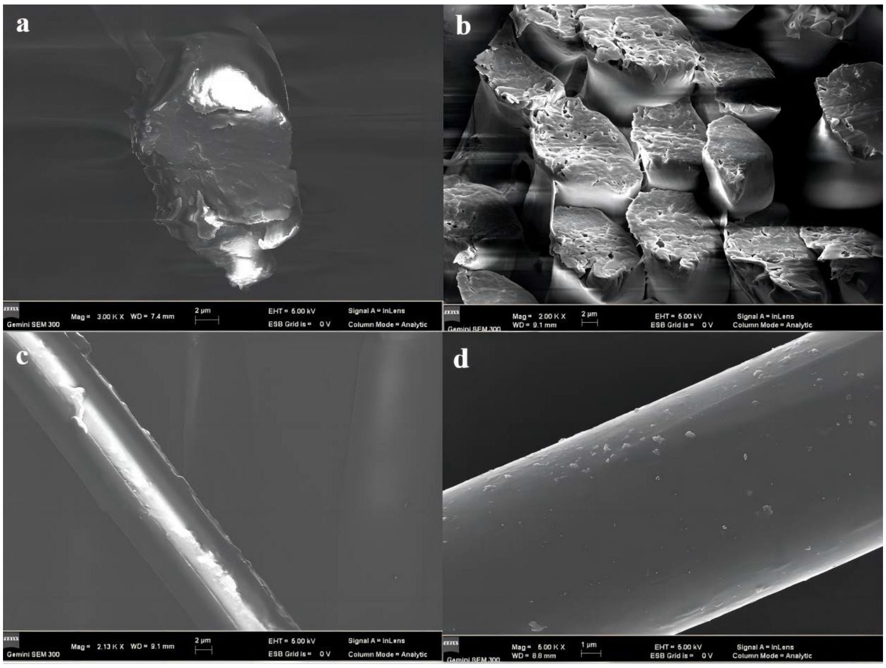

Figure 10: SEM images of neat Lyocell fibers (a, c) and functionalized Lyocell fibers (b, d)

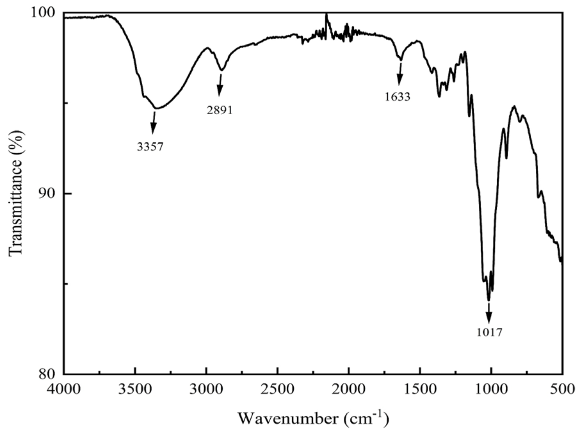

Figure 11: Infrared spectrum of functional Lyocell fiber

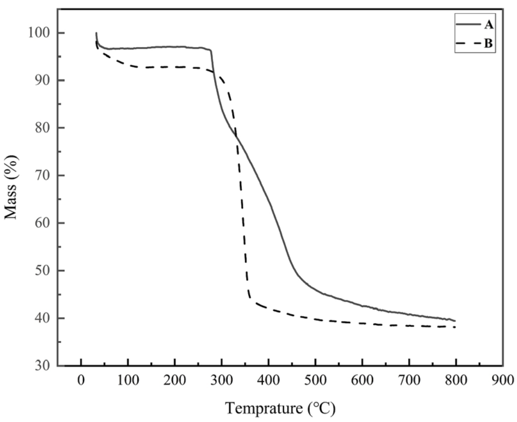

Figure 12: TG curves of neat Lyocell fiber (A) and functional Lyocell fiber (B)

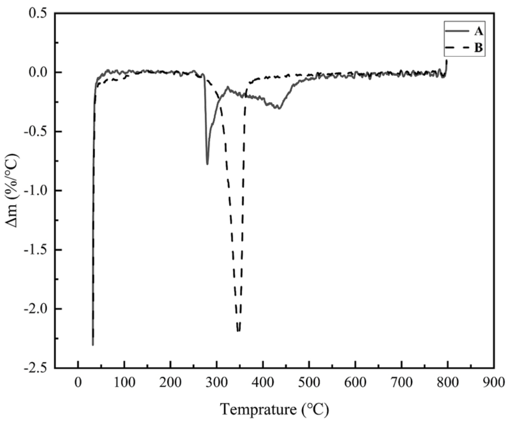

Figure 13: DTG curves of neat Lyocell fiber (A) and functional Lyocell fiber (B)

Thermogravimetric analysis

From the analysis of Figures 12 and 13, it can be seen that, in the range of 50~150 °C, the evaporation of water inside the fiber occurs; in this range, weight loss occurs faster for the functionalized Lyocell fiber than for the neat Lyocell fiber, probably because the high temperature accelerates the volatilization of nanocapsule core material and water, resulting in weight loss. The weight loss of neat Lyocell fiber starts to drop rapidly at about 240 °C. At this stage, the glycosidic bond in the cellulose macromolecule starts to break because of the heat, and the weight loss is of about 60%. The DTG curve of neat Lyocell fiber has two peaks, reflecting different steps of weight loss. At 550 °C, the fiber carbonizes. The functionalized Lyocell fiber starts thermal decomposition at a slightly higher temperature than neat Lyocell fiber – around 250 °C. The weight loss during this process is about 55%, which may be due to IPDI with cycloalkane structure, which not only makes the shell layer of CNC have a certain strength, but also forms a curing network structure in the fiber,[11] so that the heat resistance of Lyocell fiber is improved. Also, the decomposition occurs faster in the functionalized fiber compared to the neat one, probably due to the decomposition of nanocapsules. Fiber carbonization is noted at about 400 °C.

Mosquito repellence performance test

The anti-mosquito tests of the CNC functionalized Lyocell fiber revealed a mosquito repelling rate of 52.83% against *Aedes albopictus*, which meant a good repellent effect. Thus, the fibers could be ranked as belonging to category B in terms of anti-mosquito rating. The repelling property was not excellent as the CNC were partially wrapped inside the fiber, the core material was released slowly, affecting the anti-mosquito effect. Still, the CNC functionalized Lyocell fiber had good repellent effect.

In an attempt to improve the repelling effect, the CNC prepared by the optimum process was also applied directly on the Lyocell fabric by post-finishing, and its mosquito repelling property was assessed. In this case, the anti-mosquito test found that the repellency rate of *Aedes albopictus* reached 93.58%. Such a strong repellent effect ranked the fiber into category A of anti-mosquito rating.

Antibacterial performance analysis

As shown in Figure 14, antibacterial tests were performed on CO (b) and CNC (c) with deionized water (a) as the control group, and on functionalized Lyocell fibers (e), with neat Lyocell fibers (d) as the control group. The inhibition rate was calculated and the results are shown in Table 2.

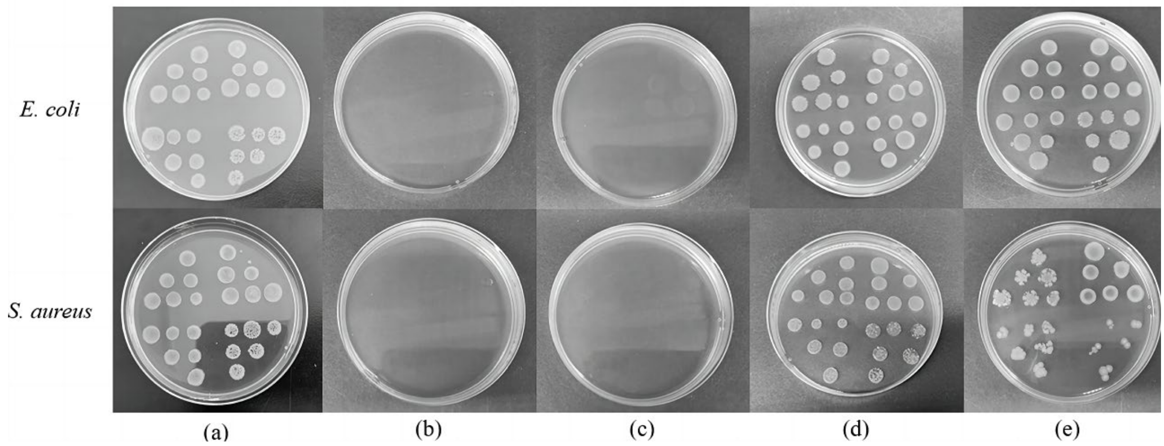

Figure 14: Antibacterial test results of different specimens ((a) deionized water as the control group, (b) CO and (c) CNC; (d) neat Lyocell fibers as the control group and (e) functionalized Lyocell fibers)

Table 2
Bacterial inhibition rate of different specimens

Specimen	Bacterial inhibition rate, %	
	E. coli	*S. aureus*
CO	99.99	99.99
CNC	99.99	99.99
Functionalized Lyocell fiber	/	97.72

As shown in Figure 14 and Table 2, the inhibition rate of CO and CNC reached 99.99% for both *E. coli* and *S. aureus*, which proves that CO and CNC have good antibacterial properties. The inhibition effect of functionalized Lyocell fibers against *E. coli* was not obvious, but the inhibition rate towards *S. aureus* reached 97.72%. It may be due to the fact that the content of CNC in functional Lyocell fibers was quite low and the content of CO was only 5%, thus, the material reached the minimum inhibitory concentration (MIC) against *S. aureus*, but not against *E. coli*. Otherwise said, functional Lyocell fibers showed a significant antibacterial effect against *S. aureus*, but not against *E. coli*.

CONCLUSION

In this study, we synthesized citronellal nanocapsules, with mosquito repellent effect by interfacial polymerization, and explored the best process conditions for their synthesis. The optimum preparation of CNC was achieved at: core to shell ratio of 6:1, CO to GTCC mass ratio of 3:1, EG dosage of 25% of the shell material, TEMED dosage of 10% of the shell material, 10% SDS solution dosage of 20%, deionized water dosage of 41.25%, emulsification time of 30 min, polymerization time of 4 h, and polymerization temperature of 60 °C. The average particle size of the CNC prepared by this process is about 200 nm, with uniform particle size distribution.

The thus-prepared CNC was added to the spinning solution of Lyocell and functionalized Lyocell fiber, with mosquito repellent and antibacterial effects, was obtained by wet spinning. The functional Lyocell fibers prepared by wet spinning with 22% CNC added to the spinning solution showed a slight improvement in heat resistance, a decrease in breaking strength and elongation at the break due to doping, compared to the neat fiber, and a grade B mosquito repellent effect and excellent inhibitory effect on *S. aureus*. The CNC was also applied directly to the fiber as a post-finish procedure and, in this case, the mosquito repellent effect of CNC functionalized Lyocell fibers ranked the fibers as belonging to grade A. The promising results obtained in in this study provide the basis for future research under realistic field conditions.

REFERENCES

[1] H. Lee, S. Halverson and N. Ezinwa, *Primary Care*, **45**, 393 (2018), https://doi.org/10.1016/j.pop.2018.05.001

[2] M. V. Reddy, S. L. Ganesan, K. Narayanan, M. Jayashree, K. Nallasamy *et al*., *Indian J. Pediatr*., **87**, 12 (2020), https://doi.org/10.1016/j.hmedic.2023.100008

[3] M. Tavares, M. R. M. da Silva, L. B. de Oliveira de Siqueira, R. A. S. Rodrigues, L. Bodjolle *et al*., *Int. J. Pharmaceut*., **539**, 190 (2018), https://doi.org/10.1016/j.ijpharm.2018.01.046

[4] C. A. Ferraz, M. R. Pastorinho, A. Palmeira de Oliveira and A. C. A. Sousa, *Environ. Pollut*., **292**, 118319 (2022), https://doi.org/10.1016/j.envpol.2021.118319

[5] C. Grison, D. Carrasco, F. Pelissier and A. Moderc, *Front. Ecol. Ecol*., **8**, 8 (2020), https://hal.science/hal-02964366

[6] Y. Zhao, Y. Wang and Z. Zhang, *Molecules*, **28**, 4979 (2023), https://doi.org/10.1016/j.jclepro.2021.126270

[7] S. A. S. Chatha, M. Asgher, R. Asgher, A. Hussain, Y. Iqbal *et al*., *Sci. Total Environ*., **690**, 2019, https://doi.org/10.1016/j.scitotenv.2019.06.520

[8] K. Kowalewska, K. Kwaczyński, M. Tarabet, K. Sobczak, A. Leniart *et al*., *Electrochim. Acta*, **468**, 14139 (2023), https://doi.org/10.1016/j.electacta.2023.143139

[9] K. J. Edgar and H. Zhang, *Carbohyd. Polym*., **250**, 116932 (2020), https://doi.org/10.1016/j.carbpol.2020.116932

[10] M. Robert M. da Silva and E. Ricci-Júnior, *Acta Trop*., **212**, 105419 (2020), https://doi.org/10.1016/j.actatropica.2020.105419